The pinch-off effect and inhomogeneous barrier height analysis in Al/p-GaAs Schottky barrier diodes

M. SOYLU[a], F. YAKUPHANOGLU[b*], W. A. FAROOQ[c]
[a]*Department of Physics, Faculty of Sciences, Bingöl University, Turkey*
[b]*Department of Metallurgical and Materials Engineering, Fırat University,23119, Elazığ, Turkey*
[c]*Department of Physics, College of Science,King Saud University, Riyadh, Kingdom of Saudi Arabia*

Al/p-GaAs Schottky barrier diodes (33 dots) were identically prepared. The effective barrier height values of one of the Al/p-GaAs Schottky barrier diodes were obtained as 0.681 and 0.945 eV from current–voltage characteristics using the thermionic emission theory and capacitance–voltage characteristics, respectively. The discrepancy between the barrier heights was explained in terms of barrier height inhomogeneity approach. It is seen that the Schottky barrier heights and ideality factors obtained from the *I-V* characteristics differ from diode to diode even if the samples are identically prepared. The origin of the barrier height inhomogeneity was analyzed by considering theoretical results obtained by Tung model. The obtained results indicate that the electron transport at the metal/semiconductor contacts are significantly affected by patches, but, the potential in front of small patches with low SBH surrounded by patches with high SBH is pinched off.

(Received January 24, 2011; accepted February 17, 2011)

Keywords: GaAs, Schottky diode, I-V and C-V measurements, Barrier inhomogeneities

1. Introduction

Gallium arsenide is one of the most popular semiconductors that has intrinsic electrical properties superior to silicon, such as a direct energy gap, higher electron mobility, a high breakdown voltage, chemical inertness, mechanical stability, and lower power dissipation. GaAs-based Schottky barrier diodes (SBDs) are used as a basic component for high-speed electronic and optoelectronic devices [1]. These advantages of gallium arsenide make it attractive for optoelectronic devices, discrete microwave devices and/or large-scale integrated electronic devices. The nature of possible conduction mechanisms has not yet been fully understood. So, it has been made many attempts to understand the nature of the conduction mechanism [2-10]. The Schottky barrier height (SBH) is an important parameter which determines the electrical characteristics of MS contacts and has crucial importance for successful operation of semiconductor devices [11–17]. The Schottky barrier height is defined as the difference between the edge of the respective majority- carrier band of the semiconductor and the Fermi level at the interface. Most of the experimental and theoretical studies have been made on the nature and formation of the barrier height at MS contacts. Schottky barrier inhomogeneity has attracted increasing attention from both scientific and technological points of view. The experimental BHs and ideality factors obtained from the *I-V* characteristics differ from diode to diode even if they are identically prepared SDs. Furthermore, there is a linear relationship between experimental effective BHs and ideality factors of Schottky contacts that can be explained by lateral inhomogeneities of the BHs in SBDs [18-21], that is, the BHs become smaller as the ideality factors increase. An investigation indicates that the experimentally observed dependence of the effective barrier heights and the ideality factors of real metal–semiconductor contacts can be explained by lateral inhomogeneities of the barrier height. The barrier heights of laterally homogeneous contacts may then be obtained by extrapolation of experimental φ_{ap} vs n relation to the corresponding image-force-controlled ideality factor n [22]. Moreover, Tung and co-workers reported theoretically [19,23] and Monch and co-workers showed experimentally [22,24-25], that a correlation exists between effective BHs and ideality factors, which may be approximated by a linear relationship. Some authors have been able to account for much of the observed non-ideal behavior by assuming certain distributions of microscopic BHs for the different diodes. Forment et al. [26] obtained an average value of 0.883 eV using BEEM to measure local BHs on a nanometer scale for Au/n-GaAs SBDs. Leroy et al. [27] measured an average BH of 0.819 eV of the whole contact for Au/n-GaAs SBDs using a conducting probe-AFM, instead of local nanometer-scale BHs. They concluded that a lower average of an effective BH was obtained due to averaging over the whole contact. In spite of the widespread literature on n-GaAs published during the last decades, theoretic analysis of the barrier

height inhomogeneity in identically prepared metal/p-GaAs Schottky barrier diodes have not studied yet.

In present work, the I–V and C–V characteristics of Al/p-GaAs (100) Schottky contacts were measured at room temperature and determined the effective barrier heights, ideality factors and series resistance to analyze the pinch-off effect and inhomogeneous barrier height analysis in Al/p-GaAs Schottky barrier diodes.

2. Experimental details

For fabrication of GaAs Schottky diodes, one side polished p-type GaAs (100) wafer having a free carrier concentration of 1.7×10^{16} cm^{-3} was used. Firstly, the wafer was ultrasonically cleaned with trichloroethylene, acetone and methanol for 5 min, respectively. The wafers rinse in de-ionized water of 18 MΩ and dry with high purity N_2. The native oxide on the surface was etched in sequence with acid solutions $(H_2SO_4 : H_2O_2 : H_2O = 3:1:1)$ for 60 seconds, and $(HCl : H_2O = 1:1)$ for another 60 seconds. Again, rinse in deionized water of 18 Mohm and dry with high purity N_2. After the etching process, the wafer was immediately inserted in to the deposition chamber. Ohmic contacts were made by evaporation of indium (In) on non-polished side of the GaAs wafer and then by thermal annealing at 350 ^{0}C for 3 minutes in flowing nitrogen in a furnace. The circular shaped Schottky metal, Al was then deposited through a molybdenum (Mo) mask by thermal evaporation. The pressure during evaporation was at about 2.6×10^{-6} mbar. Thus, Al/p-GaAs Schottky diodes were obtained. The substrate contains 33 Al/p-GaAs diodes. Current-voltage (I-V) and capacitance-voltage (C-V) measurements of the devices were made using a 4200 SCS semiconductor characterization system, at room temperature. Before the Al evaporating, the surface morphology and roughness of GaAs substrate were investigated using Park System XE-100E atomic force microscopy (AFM).

3. Results and discussion

3.1. Surface morphology of GaAs and electrical characteristics of Al/p-GaAs Schottky diode

Fig. 1 shows the AFM image of the GaAs substrate surface. The scan size of the image is 10×10 μm^2. From AFM measurements, the roughness for the GaAs substrate was found to be 11.686 nm. This means that the substrate surface has a good smooth. High flatness of the substrate surface causes high quality metal/semiconductor interface.

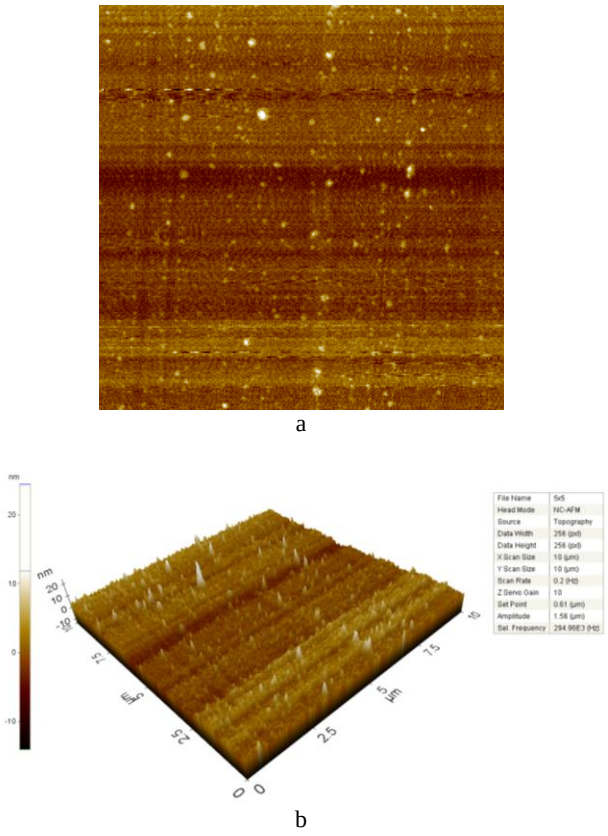

Fig. 1. AFM images of the native GaAs substrate surface a) 1D b) 3D.

Fig. 2 shows the capacitance–voltage (C–V) curve of one of the Al/p-GaAs diodes at room temperature. The capacitance of a rectifying contact can vary due to defects in semiconductor and the presence of deep lying impurities in the depletion region. The defects act either as traps or as recombination centers in the semiconductors, depending on the capture cross section of the electrons and holes. Traps reduce the semiconductor free carrier density whereas recombination centers introduce generation–recombination currents in rectifying devices. In Schottky diodes, the depletion layer capacitance can be analyzed by the following relation [28]

$$\frac{1}{C^2} = \frac{2(V_{bi} + V_r - kT/q)}{q\varepsilon_s\varepsilon_o A^2 N_i}, \qquad (1)$$

where, V_{bi} is the built-in voltage determined from the extrapolation of the $C^{-2} - V$ plot to the voltage axis, V_r is the reverse voltage, A is the area of the diode, ε_s is the static dielectric constant, $\varepsilon_o = 8.85\text{x}10^{-14}$ F/cm and N_i is the concentration of the non-compensated ionized acceptors. The N_i is related to the slope of C^{-2} vs. V curve and can be obtained from the expression given below

$$N_{\mathrm{i}} = \frac{2}{q\varepsilon_{\mathrm{s}}\varepsilon_o A^2}\left[\frac{1}{d(C^{-2})/dV}\right]. \quad (2)$$

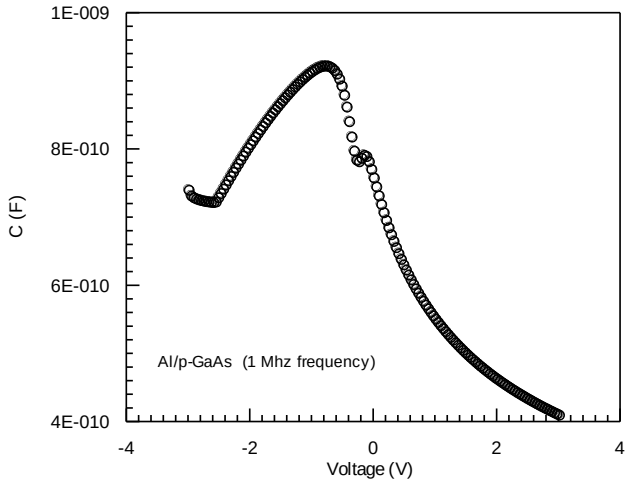

Fig. 2. The reverse bias C-V characteristic of one of the Al/p-GaAs SBDs.

The BH deduced from capacitance is then obtained from

$$\Phi_b^C = V_{\mathrm{bi}} + V_{\mathrm{n}} + \frac{kT}{q} - \Delta\phi \quad (3)$$

where V_{n}, referred to as the Fermi level potential, is the energy difference between the Fermi level and the top of the valence band, and given by $V_{\mathrm{n}} = kT/q[\ln(N_{\mathrm{v}}/N_i)]$. Thus, Eq. (3) can be rewritten by neglecting the image-force barrier lowering ($\Delta\phi$) as

$$\Phi_b^C = V_{\mathrm{bi}} + \frac{kT}{q}\left[1 + \ln\frac{N_{\mathrm{v}}}{N_{\mathrm{i}}}\right], \quad (4)$$

where N_{v} (=7.0×10^{18} cm^{-3}) is the effective density of states in valence band for p-GaAs at 300 K [29]. The V_{bi} and N_{i} values are obtained from the intercept and the slope of the extrapolated C^{-2}-V line with the V_{r} axis, respectively. Then, the value of $\Phi_{\mathrm{b}}^{\mathrm{C}}$ is calculated as 0.945 eV by using Eq. (4). The current through a Schottky barrier diode according to thermionic emission (*TE*) theory is given by the following relation [13]

$$I = I_0 \exp\left(\frac{q(V - IR_{\mathrm{s}})}{nkT}\right)\left[1 - \exp\left(-\frac{q(V - IR_{\mathrm{s}})}{kT}\right)\right] \quad (5)$$

Where, V is the applied voltage (V_{d}=V-IR$_{\mathrm{s}}$), n is the ideality factor, I_0 is the reverse saturation current given by

$$I_0 = AA^*T^2 \exp\left(-\frac{q\Phi_{\mathrm{b0}}}{kT}\right). \quad (6)$$

Where q is the electronic charge, A^* is the effective Richardson constant, k is the Boltzmann constant, T is the absolute temperature and Φ_{b0} is the zero- bias barrier height. n is the ideality factor and $\beta = \partial\Phi_b/\partial V$ is the change in the BH with bias voltage. If β is constant, n is also constant so that a plot of lnI vs. V in the forward direction should give a straight line except for the region where V<3kT/q [13]. Hence, saturation current density I_0 is derived from the intercept of the straight line in the semi-logarithmic I–V plot for zero bias and the values of Φ_b and n of a SBD can be extracted from the intercept and the slope of the linear portion of the semi-logarithmic I–V plot, respectively, Eq. (5) has the advantage that n can be found experimentally by plotting ln[I/{1−exp(qV$_{\mathrm{d}}$/kT)}] vs. V$_{\mathrm{d}}$. This plot should be a straight line of which slope q/nkT if n is constant, even for V<3kT/q. However, more usually β is not constant and the plot of ln[I/{1−exp(qVd/kT)}] vs. V$_{\mathrm{d}}$ is not linear. In this case,

$$\frac{1}{n} = \frac{kT}{q}\frac{d}{dV}\ln\left[\frac{I}{1 - \exp(qV_d/kT)}\right] \quad (7)$$

or, for V>3kT/q,

$$\frac{1}{n} = \frac{kT}{q}\frac{d(\mathrm{In}I)}{dV}. \quad (8)$$

Fig. 3 shows reverse and forward *I-V* characteristics of one of the Al/p-GaAs SBDs at room temperature. The barrier height and the ideality factor obtained from semi-logarithmic *I-V* characteristics were calculated to be 0.68 eV and 1.411, respectively. Forment et al. [26] and Leroy et al. [27] reported the average SBHs value of 0.883±0.018 eV and 0.819±0.01 eV for Au/n-GaAs, respectively. Dogan et al. [30] obtained the homogeneous SBH value of 0.862 eV for Ni/n-GaAs. Mazari et al. [31] reported the SBHs value of 0.67 eV for Al/p-GaAs prepared on the surface of the untreated p-GaAs substrate. Myburg et al. [32] prepared 13 metals on MBE grown p-GaAs. Ru had the lowest mean SBH of about 0.60 eV on p-GaAs and Ga had the highest on p-GaAs of 0.83 eV. Al had the mean SBH of 0.67 eV on p-GaAs. The obtained barrier height of the studied diode is in close agreement with the values reported in literature.

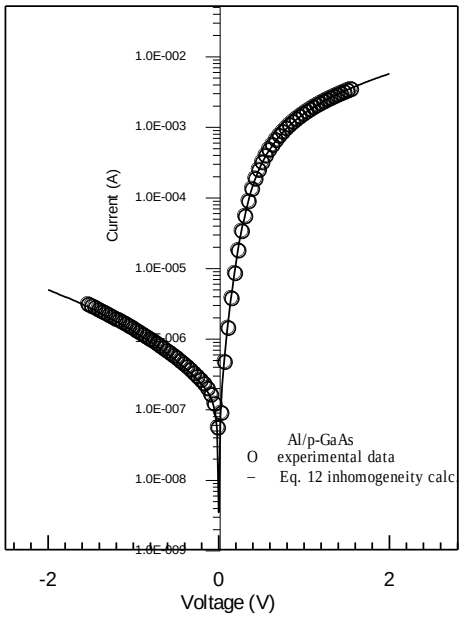

Fig. 3. Experimental forward and reverse bias current vs voltage characteristics of one of the p-GaAs SBDs at room temperature. The full line is a fit of Eq. (12) to the experimental data.

The barrier height value obtained from the reverse bias C–V characteristic is different that of obtained from the I–V characteristics. That is, the BH (C–V) value is obtained higher than the BH (I–V) value due to the barrier inhomogeneities and distributions of the interfacial charges. Since the C-V technique yields an average SBH for the whole diode, the experimentally observed dependence of SBH on the measurement technique is likely due to a distribution of SBHs. Furthermore, this also shows that the I–V and C–V characteristics have different nature [7,33]. The C-V measured BH, on the other hand, is influenced by the distribution of charge at the depletion region boundary. There have also been some reports showing that the discrepancy between BHs measured by different techniques might be associated with the instrumentation problems; namely, the way to determine true space-charge capacitance from C–V data or a large series resistance, which could affect the value determined from *I–V* data [19,34]. The difference between barrier heights obtained from I–V to C–V measurements for the Al/p-GaAs SBDs may be explained by existence of SBH inhomogeneity on MS contacts, as will discuss below.

The I-V characteristics deviate from linearity due to the series resistance and interfacial layer. Thus, the series resistance is effective parameter in I-V characteristics of the diode and it can not be ignored. We have used Norde's functions [18] to obtain the value of the series resistance. The F(V) function is defined as

$$F(V) = \frac{V_0}{\gamma} - \frac{kT}{q}\left(\frac{I(V)}{A^* AT^2}\right), \qquad (9)$$

where γ is the first integer (dimensionless) greater than n. Here, it has been taken as 2. I(V) is the current obtained from the I–V characteristics of the diode. The plot of F(V) vs voltage for the diode is shown in Fig. 4. The F(V) gives a minimum point and thus, the barrier height and the series resistance for the diode is calculated by the relation,

$$\Phi_b = F(V_0) + \frac{V_0}{\gamma} - \frac{kT}{q}, \quad R_s = \frac{kT(\delta - n)}{qI_o} \qquad (10)$$

Where $F(V_o)$ is the minimum point of F(V) and V_0 is the corresponding voltage. Using Eq. 10, the barrier height and the R_s value for the diode were found to be 0.72 eV and 0.919 kΩ, respectively. The series resistance causes a non-linear region of forward bias I–V curve of the diode.

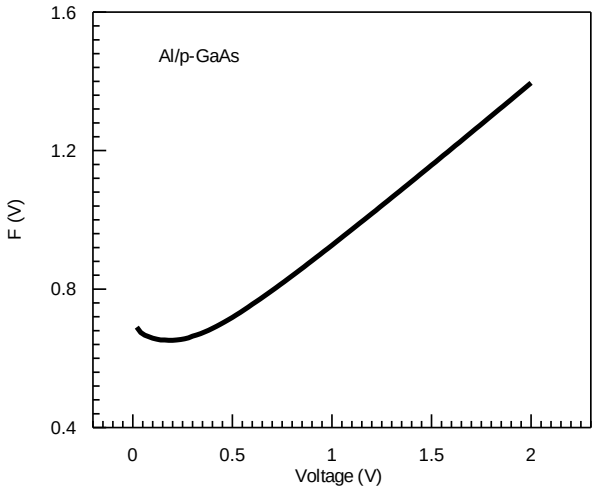

Fig. 4. F(V) vs. V plot of the Al/p-GaAs Schottky diode.

Furthermore, the barrier heights Φ_{b0} for identically prepared the Al/p-GaAs SBDs were varied from 0.582 to 0.681 eV and the ideality factors were varied from 1.411 to 2.12. The obtained results indicate that the experimental BHs and ideality factors obtained from the *I-V* characteristics can differ from diode to diode even if they were identically prepared on the same sample. Fig. 5 shows a plot of the Φ_{b0} vs. *n* of identically prepared Al/p-GaAs SBDs at room temperature. It was seen that ideality factors were decreased, while the BHs were increased or vice versa due to inhomogeneities. The straight line in Fig. 5 is the least-square fitting to the experimental data. As seen in this figure, there is a linear relationship between Φ_{b0} and *n* parameters of Al/p-GaAs Schottky contacts. This finding may be attributed to lateral inhomogeneities of the BHs in Schottky diodes [19,23,24,35–41]. In addition, it has been mentioned by Tung and co-workers [19,23] and Mönch and co-workers [34–37] that higher ideality factors among identically prepared diodes were often found to accompany lower observed BHs. Due to lateral inhomogeneities of the BH, both parameters differ from one diode to another. However, their variations are correlated in that Φ_{b0} becomes smaller with increasing *n*.

Extrapolations of such Φ_{b0} vs n plots to the corresponding image-force-controlled ideality factors n_{if} give the BHs of laterally homogeneous contacts. They are then compared with the theoretical predictions for ideal Schottky contacts. The observation of large ideality factors when the diode is in a state of maximum confusion is in good agreement with the interpretation of ideality factors based on SBH inhomogeneity. There are certainly other sources for SBH inhomogeneity which may be imagined. For example, there may be a mixture of different metallic phases with different SBHs at a MS interface due to incomplete interfacial reaction. Additionally, there may be doping inhomogeneity at the MS interface and dopant clustering. The contamination at a MS interface is often present at the MS interfaces of diodes prepared by the routine processing methods used in the semiconductor electronics industries. These contaminants may act directly to introduce inhomogeneity or they may simply promote inhomogeneity, through the generation of defects, additional interfacial chemical phases, etc. Even in the absence of chemical contaminants, SBH inhomogeneity may be present. Thus, interface roughness may contribute to the presence of SBH inhomogeneity, due to effectively increasing or decreasing the low-SBH patches. Finally, there are numerous structural defects, grain boundaries, dislocations, stacking faults, at MS interfaces, and these may contribute to SBH inhomogeneity [23].

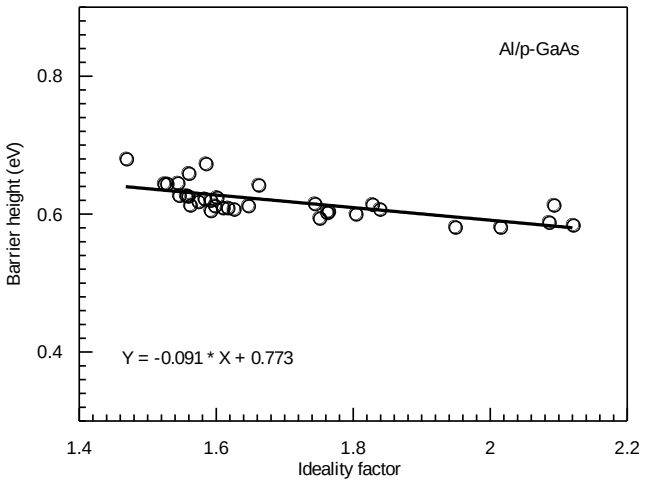

Fig. 5. Experimental barrier height vs ideality factor plot of Al/p-GaAs SBDs at room temperature.

The current in the I-V measurement is dominated by the current which flows through the region of low SBH. Schmitsdrof et al. [42] have justified this procedure by numerical simulations of *I-V* curves which use Tung's theory of laterally inhomogeneous contacts with Gaussian distributions of the parameter characterizing such patchy metal-semiconductor interfaces. These results suggest that the formation mechanism of the SB is locally non-uniform at common [19,42]. Furthermore, the reason of low BHs and high *n* values in inhomogeneity model based on small local regions or patches with lower BH than the junction's main BH assumed to exist at the junction may be explained by the patch density. According to the investigations by Schmitsdrof et. al [42], the larger the patch density and/or the standard deviation of the patch-parameter is, the larger the respective ideality factor is. So, it has been speculated that the reason of the experimentally observed reduction of the BHs with increasing ideality factors is inhomogeneity of the contact comprises patches with smaller BHs. Therefore, the ideality factors represent a direct measure of the interface uniformity. Tung [43] has treated the SBH inhomogeneity to account for local variations in transport properties. In this model, when the regions of low SBH are comparable to or smaller than the semiconductor depletion width *w*, the conduction path in front of this patch becomes frequently ''potentially pinched-off'' by the surrounding high barrier region. "Pinch off" is a concept often used to describe the operation of a field effect transistor. The condition for pinch off is given by [19]

$$\Delta / V_{bb} > 2R_0 / w \tag{11}$$

Where Δ, V_{bb} , R_0, w are the barrier height reduction at the interface of the patch compared to the homogeneous value, the interface band bending of the uniform barrier outside the patches, the radius of a circular patch, the depletion layer width, respectively.

The total current through the inhomogeneous MS contact which exhibit circular patches with Gaussian distribution of the patch parameter $\gamma = 3(R_0^2\Delta/4)^{1/3}$ is given by [19]

$$I = AA^*T^2 \exp(-\Phi_{b0}^{\text{hom}}/kT)[\exp(q(V - IR_s)/kT) - 1](1 + J) \tag{12}$$

The total junction current is made of two terms. One of which is the characteristic of the current through the whole area with a uniform SBH. The other additional current term J is current through the patches. The patch function J can be expressed as

$$J = \frac{AA_{eff}\rho}{(IRs - V)^{1/3}} \exp[\frac{q^2\sigma^2(V_{b0} - V + IR_s)^{2/3}}{2k^2T^2\eta^{2/3}}] \tag{13}$$

Where σ is standard deviation of $\gamma \geq 0$, $A_{eff} = (8\pi\sigma^2/9)(\eta/V_{b0})^{1/3}$, $\eta = \varepsilon_s\varepsilon_0/qN_d$ and V_{b0} is the interface band bending of the uniform barrier. Thus, Eq. (12) completely describes the current through inhomogeneous Schottky contacts that exhibit circular patches with a Gaussian distribution of the patch parameter. The diode current predicted by Eq. (12) shows a variety of the experimental forward and reverse I–V data. As can be seen from Fig. 3, there is excellent agreement between the experimental data and the fitted curve. This means that the experimental data are very well described by the pinch-off theory of Tung. We have obtained a homogeneous barrier height Φ_{hom}=0.745 eV, a Standard deviation of the patch parameter σ=3.4x10^{-5}

$cm^{2/3}V^{1/3}$ (the standard deviation of patch parameter γ), a patch density ρ=6.2×10^{12} cm^{-2}, a series resistance R_s= 0.919 kΩ by using N_a=1.7×10^{16} cm^{-3}, V_{b0}=0.411 V, A=0.031 cm^2 and T=296 K for the Al/p-GaAs SBD.

The combined effect of all the low SBH patches is as if there were a big low SBH region in the diode with an effective area and effective SBH in an inhomogeneous SBD is given by [19]

$$\Phi_{eff} = \Phi_{b0}^{\hom} - (\Delta\Phi),$$
$$\Delta\Phi = \sigma^2 / 2kT)(V_{b0} / \eta)^{2/3} \quad (13)$$

For a current described by Eq. (12), the ideality factor is given by [19]

$$n \approx 1 + \Gamma, \quad \Gamma \approx \frac{\sigma^2 V_{b0}^{-1/3}}{3kT\eta^{2/3}} \quad (14)$$

From above equation $\Delta\Phi$, patch radius and Γ are 0.254 eV, 36.75 nm, 0.411, respectively. Furthermore, the value of n = 1.411 (1+0.411=1.411) from the fitting the parameters is the same as the value of 1.411 obtained from the experimental I–V characteristics for the Al/p-GaAs SBD. This patch radius value is 15.47 % of the depletion layer width in the homogeneous regions. Leroy et al. [27] have obtained a patch radius value for Au/n-GaAs SBDs what is equivalent to 8 % of the depletion layer width w in the homogeneous regions. It has been found to be 24.74 % of the depletion layer width in the homogeneous regions in ref. [44]. Thus, it has been also achieved the characterization of the patches with lower BH. The potential distribution also varies from region to region if the SBH varies locally at Al/p-GaAs interface. The potential in front of a small area with low SBH is easily "pinched off" if surrounded by regions with high-SBH. The potential distribution of low SBH circular patches is given by [19]

$$V(0,z) = V_{bb}(1-\frac{z}{w})^2 + V_n + V_a - \Delta\Phi[1-\frac{z}{(z^2+R_0^2)^{1/2}}]. \quad (15)$$

Where w is depletion width and z is depth from surface. In Fig. 6, the potential distributions along V=0.0 V of 1ow SBH circular patches are plotted for patches with different Δ's. For a large Δ, the potential in front of the patch is obviously pinched off. The larger Δ is, the greater is the degree of pinch-off. Pinch-off of the low-SBH patch only occurs when Δ is larger than $\Delta_{crit.}$. In this study, we estimate that the critical value for potential pinch-off is about 0.128 eV using equation (11). The experimental value of Δ obtained for the Al/p-GaAs SBD is larger than the critical value. Thus, there is pinch-off effect. The potential distributions of 1ow SBH circular patches are plotted for patches with different radius R_0 in Fig. 7. The slope at the small value of z for the potential distribution is positive. For a small R_0, the potential in front of the patch is obviously pinched off, that is, while the low-SBH patch radius decreases, the patches become more pinched-off and the potential at the saddle point increases. The low patch radius value of 36.75 nm is due to the doping level of substrate and standard deviation value of σ=3.4×10^{-5} $cm^{2/3}V^{1/3}$. Furthermore, the dependence of the potential on the applied bias has a very important effect on conduction mechanism at inhomogeneous SBDs. The potential barrier between the metal and the semiconductor increases with forward bias and decreases with reverse bias [19,23]. In Fig. 8, the potential distributions of a circular patch of low SBH are shown for different voltage biases across the Al/p-GaAs contact. The dependence of the potential on the applied bias has a very significant impact on transport properties at inhomogeneous SBDs. As seen in Fig. 8, the saddle-point potential slowly rises with forward bias and slowly decreases with reverse bias. Since the effective barrier height of the low-SBH region is due to the magnitude of the potential at the saddle point, a variation in the potential at the saddle point with bias implies a variation in effective SBH with bias. To investigate the influence of the patch density on the conduction mechanism and BH homogeneity, it has been varied the patch density keeping the other parameters. The simulated I-V characteristics of the patch density are shown in Fig. 9. The values of patch density of an inhomogeneous Al/p-GaAs SBD with $\Phi_b^{\hom}$=0.68 eV, R_s=0.919 kΩ, σ=3.4×10^{-5} $cm^{2/3}V^{1/3}$, A=0.031 cm^2 and T=296 K were varied from 0.4×10^{12} cm^{-2} to 16.4×10^{12} cm^{-2}. These curves approximately reach the saturation at the value of 6.2×10^6 cm^{-2}. The obtained plots demonstrate that the electron transport at the metal/semiconductor contacts is significantly affected by the patch density. In Fig. 10, the potential distributions along of a circular patch of low SBH are shown as a function of the substrate doping level. The condition set by eq. (11) demonstrates that potential pinch off is most dominant when the SC doping level is low and the low SBH patch is small. As seen in Fig. 10, when the substrate doping is low, the magnitude of the potential at the saddle point is high. It means that the low-SBH patch is more pinched-off or vice versa due to the substrate doping. Thus, it can be said that discrepancies between I-V and C-V measurements becomes less at lower doping levels. Furthermore, as the doping level decreases the depletion width becomes much larger than the low-SBH patch radius, and the potential in the neighborhood of the low-SBH patch becomes more pinched-off. This shows that the degree of SBH fluctuation is always significantly reduced on lightly doped semiconductors. Consequently, it is concluded that the most information about SBH inhomogeneity may be obtained from heavily doped semiconductors [23].

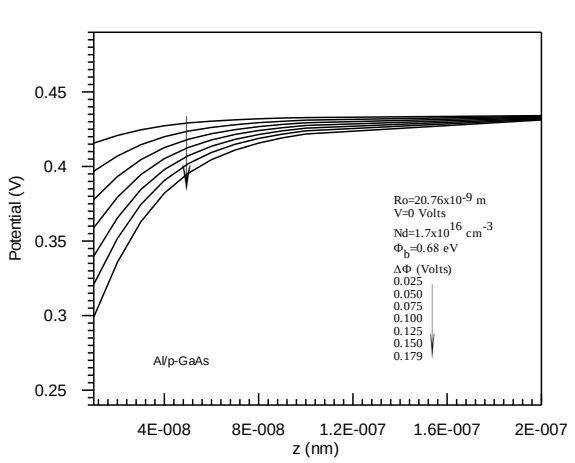

Fig. 6. The potential of the conduction-band minimum of the semiconductor for patch with SBH differences as a function of the distance z from the MS interface to the inside of the semiconductor.

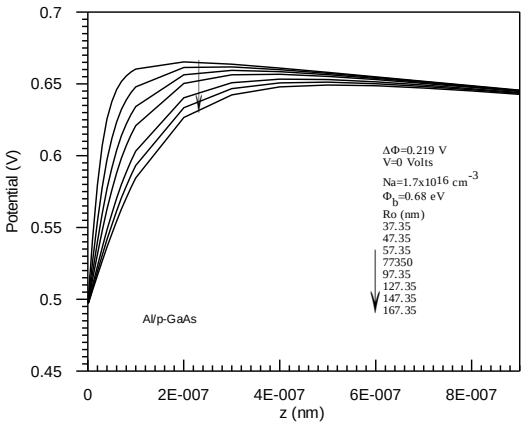

Fig. 7. The potential of the conduction-band minimum of the semiconductor as a function of the distance z, calculated with Eq. 15, illustrating the influence of the radius of a low-SBH patch on potential pinch-off.

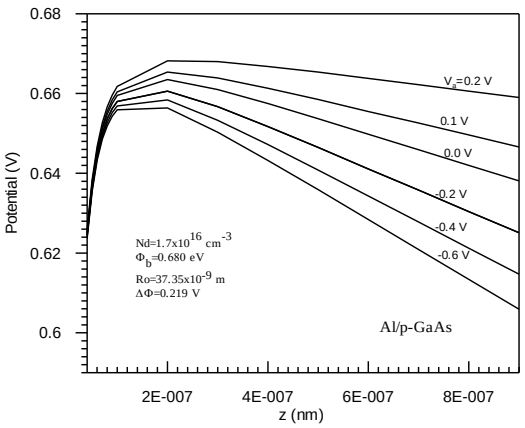

Fig. 8. The variation of the potential of the conduction-band minimum as a function of the distance z with the applied bias for a low-SBH circular patch.

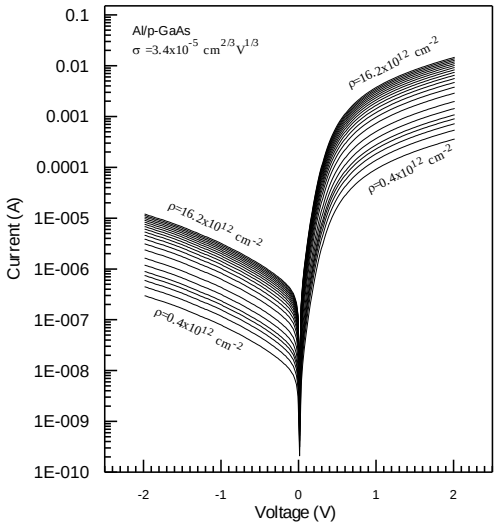

Fig. 9. The forward and reverse bias I-V characteristics, calculated using eq. 12 of an inhomogeneous Al/p-GaAs SBD.

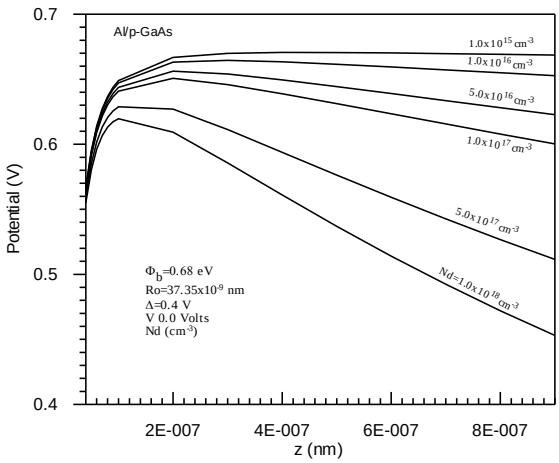

Fig. 10. Potential distributions of the low-SBH patch for various substrate doping levels.

4. Conclusions

We have investigated characteristic parameters and the BH inhomogeneity of the Al/p-GaAs SBDs which prepared on the same surface. We have shown that they reveal different BHs and ideality factors even though diodes have identically been prepared. The barrier heights obtained from I–V to C–V measurements are not the same. The discrepancy between the barrier heights determined from I–V and C–V may be explained in terms of inhomogeneity SBH approach. SBHs have been interpreted on the basis of Tung's theoretical model which assumes the existence of barrier height inhomogeneity at the metal–semiconductor interface. Tung's theory has been applied the experimental data for total thermionic emission current including a patch function describing the inhomogeneities. It has been investigated whether or not the regions of low SBH is pinched off. Our results demonstrate that the electron transport at the

metal/semiconductor contacts are significantly affected by patches, but, the potential in front of small patches with low SBH surrounded by patches with high SBH is pinched off.

Acknowledgments

This work was supported by King Saud University under grant: KSU-VPP-102 and Feyzi AKKAYA Scientific Activates Supporting Fund (FABED). One of author wishes to thank KSU and FABED for young scientist grant.

References

[1] M. G. Kang, H. H. Park, Vacuum **67**, 91 (2002).
[2] J. H. Werner, H. H. Guttler, J. Appl. Phys. **69**, 1522 (1991).
[3] J. L. Freeouf, Appl. Phys. Lett. **41**, 285 (1982).
[4] I. Ohdomari, T. S. Kuan, K. N. Tu, J. Appl. Phys. **50**, 7020 (1979).
[5] I. Ohdomari, H. Aochi, Phys. Rev. B **35**, 682 (1987).
[6] I. Bastys, V. B. Bikbaev, J. J. Vaitkus, S. C. Karpinskas, Litov. Fiz. Sb. **28**, 191 (1988).
[7] Y. P. Song, R. L. Van Meirhaeghe, W. H. Laflere, F. Cardon, Solid-State Electron. **29**, 633 (1986).
[8] S. Chand, J. Kumar, Semicond. Sci. Technol. **10**, 1680 (1995).
[9] S. Chand, S. Bala, Appl. Surf. Sci. **252**, 358 (2005).
[10] E. Dobrocka, J. Osvald, Appl. Phys. Lett. **65**, 575 (1994).
[11] S. M. Sze, Physics of Semiconductor Devices, Wiley, NewYork, 1981.
[12] C. W. Wilmsen, Physics and Chemistry of III–V Compound Semiconductor Interfaces, Plenum Press, NewYork, 1985.
[13] E. H. Rhoderick, R. H. Williams, Metal–Semiconductor Contacts, Oxford, Clarendon, 1978.
[14] L. Rideout, Thin Solid Films **48**, 261 (1978).
[15] Z. S. Horvath, J. Vac. **46**, 963 (1995).
[16] M. Soylu, B. Abay, Microelectronic Engineering **86**, 88 (2009).
[17] L. J. Brillson, Contacts to the Semiconductor, Noyes, New Jersey, 1993.
[18] H. Norde, J. Appl. Phys. **50**, 5052 (1979).
[19] R. T. Tung, Phys. Rev B. **45**, 13509 (1992); R. T. Tung, Mater. Sci. Eng. R. **35**, 1-138 (2001).
[20] F. A. Padovani, in: R. K. Willardson, A. C. Beer (Eds.), Semiconductors and Semimetals Vol. 7A Academic Pres, New York, 1971.
[21] C. R. Crowell Solid-State Electronics **20**, 171 (1977).
[22] R. F. Schmitsdorf, T. U. Kampen, W. Monch, J. Vac. Sci. Technol. B, **15**, 1221 (1997).
[23] J. P. Sullivan, R. T. Tung, M. R. Pinto, W. R. Graham, J Appl Phys. **70**, 7403 (1991).
[24] W. Monch, J Vac Sci Technol B, **17**, 1867 (1999).
[25] R. F. Schmitsdorf, W. Monch Eur Phys J B **7**(3), 457 (1999).
[26] S. Forment, R. L. Van Meirhaeghe, A. De Vrieze, K. Strubbe, W. P. Gomes, Semicond. Sci. Technol. **16**, 975 (2001).
[27] W. P. Leroy, K. Opsomer, S. Forment, R. L. Van Meirhaeghe, Solid State Electron. **49**, 878 (2005).
[28] A. Vander Ziel, Solid State Physical Electronics, 2nd edn, Prentice-Hall, Englewood Cliffs, NJ, 1968.
[29] A. Neamen Donald, in: Semiconductor Physics and Devices, Irwin, Boston, 1992; C. W. Wilmsen, Physics and Chemistry of III–V Compound Semiconductor Interface, Plenum, New York, 1985.
[30] H. Dogan, H. Korkut, N. Yıldırım, A. Turut Applied Surface Science **253**, 7467 (2007).
[31] H. Mazari, Z. Benamara, O. Bonnaud, R. Olier, Materials Science and Engineering B **90**, 171 (2002).
[32] G. Myburg, F. D. Auret, W. E. Meyer, C. W. Louw, M. J. van Staden, Thin Solid Films **325**, 181 (1998).
[33] E. H. Nicollian, A. Goetzberger, Appl. Phys. Lett. **7**, 216 (1965).
[34] W. Monch, Appl. Phys. Lett.**72**, 1899 (1998).
[35] W. Mönch, Phys. Rev. B. **37**, 7129 (1988).
[36] W. Mönch, Semiconductor Surfaces and Interfaces, third ed., Springer, Berlin, **421**, 485, 389 (2001).
[37] T. U. Kampen, W. Mönch, Surf. Sci. **331–333**, 490 (1995).
[38] K. Akkılıc, M. E. Aydın, A. Turut, Physica Scripta **70**, 364 (2004).
[39] S. M. Sze, Physics of Semiconductor Device second ed., 245 New York, Wiley, 1981.
[40] S. Zhu, X. P. Qu, V. Meirhaeghe, C. Detavernier, G. P. Ru, F. Cardon, B. Z. Li, Solid State Electron. **44**, 2217 (2000).
[41] M. Biber, O. Güllü, S. Forment, R. L. Van Meirhaeghe, A. Turut, Semicond. Sci. Technol **21**, 1–5 (2006).
[42] R. F. Schmitsdrof, T. U. Kampen, W. Mönch, J. Vac. Sci. Technol. B **15**, 1221 (1997).
[43] R. T. Tung, Appl. Phys. Lett. **58**, 2821 (1991).
[44] M. Soylu, F. Yakuphanoglu, J. Alloys Compd. **506**, 418 (2010).

*Corresponding author: fyhanoglu@firat.edu.tr, fyakuphanoglu.v@ksu.edu.sa